
HINT: Hierarchical Invertible Neural Transport for General and Sequential Bayesian inference

Gianluca Detommaso^{1,*}, Jakob Kruse^{2,*}, Lynton Ardizzone², Carsten Rother², Ullrich Köthe², and Robert Scheichl²

¹University of Bath (UK), ²Heidelberg University (GER), *co-first authors

Abstract

In this paper, we introduce Hierarchical Invertible Neural Transport (HINT), an algorithm that merges Invertible Neural Networks and optimal transport to sample from a posterior distribution in a Bayesian framework. This method exploits a hierarchical architecture to construct a Knothe-Rosenblatt transport map between an arbitrary density and the joint density of hidden variables and observations. After training the map, samples from the posterior can be immediately recovered for any contingent observation. Any underlying model evaluation can be performed fully offline from training without the need of a model-gradient. Furthermore, no analytical evaluation of the prior is necessary, which makes HINT an ideal candidate for sequential Bayesian inference. We demonstrate the efficacy of HINT on two numerical experiments.

1 Introduction

Bayesian inference is a statistical inference framework where a *prior* probability distribution of some unknown variable gets updated as more observations become available. The task of sampling from such a *posterior* probability distribution can be extremely challenging, in particular when the unknown variable is either very high-dimensional, or the underlying model is very complex and expensive to evaluate (e.g. chaotic dynamical systems, SDEs, PDEs). The problem becomes even harder when observations arrive in a streaming form and Bayesian inference has to be performed *sequentially* (a.k.a. filtering). Standard attempts to solve these tasks include MCMC algorithms, SMC techniques, variational inference approximations [12, 10, 2] and many remarkable improvements of these contributions have been proposed in the last decades.

A more recent approach entails the use of optimal transport [25] in order to map a reference density (e.g. Gaussian) to a target density (e.g. posterior) [20]. One can define a possible class of transport maps and, within this class, seek for an optimal map such that the correspondent push-forward density of the reference approximates the target as closely as possible. Samples from the target density can then be recovered by applying the transport map to samples from the reference density. The class of transport maps that is chosen characterizes the method in use. For example, [20] introduces polynomial maps within a Knothe-Rosenblatt rearrangement structure, whereas [19, 4] exploit variational characterizations embedded in a RKHS.

In this paper, we propose different ways to use Invertible Neural Networks (INNs) within an optimal transport perspective. INNs have recently been introduced in [8] as class of neural networks characterized by an invertible architecture. Crucially, every layer combines orthogonal transformations and triangular maps, which ensures that the determinant of the Jacobian of the overall map can be computed at essentially no extra cost during the forward pass. Here, we extend the results in [8, 1] and we introduce and compare different transport constructions with the goal of sampling from a posterior distribution. Finally we propose HINT, a *Hierarchical Invertible Neural Transport* method where a

hierarchical INN architecture is exploited within a Knothe-Rosenblatt structure in order to densify the input-to-output dependence of the transport map and to allow sampling from the posterior. One of the advantages of HINT is that model evaluations can be performed fully offline and the gradient of the model is not required, which is very convenient when models and their gradients (e.g. PDEs and their adjoint operators) are very expensive to compute. In addition, analytical evaluations of the prior density are never required, which makes HINT ideal for Sequential Bayesian inference.

The paper is organized as follows. Section 2 gives a background on INNs. Section 3 provides a transport perspective, where new constructions are derived and studied. Section 4 introduces HINT, a novel hierarchical architecture, and how to use it to sample from the posterior. Section 5 describes HINT in a sequential Bayesian framework. Section 6 studies the performance of the algorithm on two challenging inference problems. We finish with some conclusion in section 7.

2 Background on Invertible Neural Networks

Invertible Neural Networks (INNs) have been introduced in [8] as a special case of deep neural networks whose architecture allows for trivial inversion of the map from input to output. One can describe an INN as an invertible map $T : \mathcal{X} \rightarrow \mathcal{X}$ defined on some vector space \mathcal{X} , characterized by the composition of invertible layers T_ℓ , i.e. $T(\mathbf{u}) := T_L \circ \dots \circ T_1(\mathbf{u})$, for $\mathbf{u} \in \mathcal{X}$ and $\ell = 1, \dots, L$. The architecture of each layer T_ℓ can be described as follows:

$$T_\ell(\mathbf{u}) := \begin{bmatrix} T_\ell^1(\tilde{\mathbf{u}}_1) \\ T_\ell^2(\tilde{\mathbf{u}}_1, \tilde{\mathbf{u}}_2) \end{bmatrix} := \begin{bmatrix} \tilde{\mathbf{u}}_1 \\ \tilde{\mathbf{u}}_2 \odot \exp(s_\ell(\tilde{\mathbf{u}}_1)) + t_\ell(\tilde{\mathbf{u}}_1) \end{bmatrix}, \quad \text{with } \tilde{\mathbf{u}} := \begin{bmatrix} \tilde{\mathbf{u}}_1 \\ \tilde{\mathbf{u}}_2 \end{bmatrix} := Q_\ell \mathbf{u}, \quad (1)$$

where $T_\ell = [T_\ell^1, T_\ell^2]$ is an arbitrary splitting, $\exp(\cdot)$ denotes element-wise exponential operation, Q_ℓ are orthogonal matrices, i.e. $Q_\ell^\top Q_\ell = I$, and s_ℓ, t_ℓ are arbitrarily complex neural networks. In practice, we will take Q_ℓ to be series of Householder reflections and s_ℓ, t_ℓ as sequences of fully-connected layers with leaky ReLU activations. We denote by $\theta \in \mathbb{R}^n$ all the parameters within s_ℓ and t_ℓ that we want to learn across all layers, which will in turn parametrize the map $T(\mathbf{u}) = T(\mathbf{u}; \theta)$.

We emphasize that each layer T_ℓ is a composition of an orthogonal transformation and a triangular map, where the latter is better known in the field of transport maps as *Knothe-Rosenblatt rearrangement* [20]. This factorization can be seen as a non-linear generalization to a classic QR decomposition [24]. Whereas the triangular part encodes the possibility to represent non-linear transformations, the orthogonal part reshuffles the entries to foster dependence of each part of the input to the final output, thereby drastically increasing the representation power of the map T .

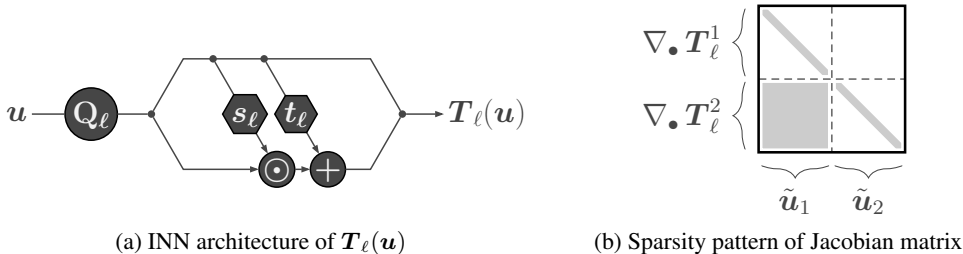
Figure 1a displays the architecture introduced in (1) corresponding to the map T_ℓ and Figure 1b the layout of the Jacobian matrix $\nabla_{\tilde{\mathbf{u}}} T_\ell$. We have the following Lemma.

Lemma 1. *Let us call $\mathbf{u}^0 := \mathbf{u} \in \mathcal{X}$, $\mathbf{u}^\ell := T_\ell(\mathbf{u}^{\ell-1})$ and $\tilde{\mathbf{u}}^\ell := Q_\ell \mathbf{u}^\ell$. Then*

$$\log |\det \nabla T(\mathbf{u})| = \sum_{\ell=1}^L \text{sum}(s(\tilde{\mathbf{u}}_1^\ell)), \quad (2)$$

where $\text{sum}(\cdot)$ denotes the element-wise sum.

A proof is given in appendix A. Lemma 1 crucially shows that the determinant of the Jacobian of an INN can be calculated for free during the forward pass. The importance of this will become clear in Section 3.



We remark that the expressions in (1) are trivially invertible:

$$\mathbf{S}_\ell(\mathbf{v}) := \begin{bmatrix} \mathbf{S}_\ell^1(\mathbf{v}_1) \\ \mathbf{S}_\ell^2(\mathbf{v}_1, \mathbf{v}_2) \end{bmatrix} := \mathbf{Q}_\ell^\top \begin{bmatrix} \mathbf{v}_1 \\ (\mathbf{v}_2 - \mathbf{t}_\ell(\mathbf{v}_1)) \odot \exp(-\mathbf{s}_\ell(\mathbf{v}_1)) \end{bmatrix}, \quad \text{with } \mathbf{v} := \begin{bmatrix} \mathbf{v}_1 \\ \mathbf{v}_2 \end{bmatrix} \in \mathcal{X}, \quad (3)$$

where $\mathbf{S}_\ell = [\mathbf{S}_\ell^1, \mathbf{S}_\ell^2]$ corresponds to the splitting of \mathbf{T}_ℓ . Note that \mathbf{s}_ℓ and \mathbf{t}_ℓ do not need to be invertible.

3 A transport perspective for general Bayesian inference

In [1], INNs were used to sample from a posterior probability distribution. In this section, we will generalize the results in [1] via the mathematical framework of transport maps. We will suggest different procedures and architectures which involve INNs and we will propose a new algorithm to perform sampling from a posterior distribution.

3.1 A general Bayesian framework

Let us denote by $\mathbf{x} \in \mathbb{R}^d$ some hidden parameters of interest and by $\mathbf{y} \in \mathbb{R}^m$ some observations. We respectively denote by $p_x(\mathbf{x})$, $p_{y|x}(\mathbf{y}|\mathbf{x})$, $p_{y,x}(\mathbf{y}, \mathbf{x})$ and $p_y(\mathbf{y})$ the prior density, the likelihood function, the joint density and the evidence. By Bayes' theorem, the posterior density can be expressed as $p_{x|y}(\mathbf{x}|\mathbf{y}) = p_x(\mathbf{x}) p_{y|x}(\mathbf{y}|\mathbf{x}) / p_y(\mathbf{y})$.

All the results we will present hold for any possible likelihood function $p_{y|x}$, in contrast with the results in [1] which hold exclusively for the Dirac delta likelihood $p_{y|x}(\mathbf{y}|\mathbf{x}) = \delta_{\mathbf{F}(\mathbf{x})}(\mathbf{y})$, where $\mathbf{F} : \mathbb{R}^d \rightarrow \mathbb{R}^m$ is some non-linear operator. However, for sake of clarity, throughout the paper we will focus on additive Gaussian noise relations, i.e. $\mathbf{y} := \mathbf{F}(\mathbf{x}) + \sigma_y \boldsymbol{\xi}$, for some standard Gaussian noise $\boldsymbol{\xi} \sim \mathcal{N}(\mathbf{0}, \mathbf{I})$ and standard deviation σ_y . It immediately follows that $p_{y|x}(\cdot|\mathbf{x}) = \mathcal{N}(\mathbf{F}(\mathbf{x}), \sigma_y^2 \mathbf{I})$.

Furthermore, we introduce a latent variable \mathbf{z} , whose dimension will be specified below. Although any treatable density can be chosen for \mathbf{z} , we will practically use a standard Gaussian $p_z = \mathcal{N}(\mathbf{0}, \mathbf{I})$.

3.2 A transport perspective

Suppose that we want to approximate a target density p_{target} . A possible approach is to seek for an invertible transport map $\mathbf{T} : \mathcal{X} \rightarrow \mathcal{X}$ such that the pushforward density $\mathbf{T}_{\#} p_{\text{ref}}$ of some reference density p_{ref} approximates, in some sense, the target p_{target} .¹ We restrict the attention to parametric families of transport maps $\mathbf{T}(\cdot) = \mathbf{T}(\cdot; \boldsymbol{\theta})$, for $\boldsymbol{\theta} \in \mathbb{R}^n$. We define the function

$$J : \mathbb{R}^n \rightarrow [0, \infty) : \boldsymbol{\theta} \mapsto \mathcal{D}_{\text{KL}}(\mathbf{T}_{\#} p_{\text{ref}} \parallel p_{\text{target}}), \quad (4)$$

where $\mathcal{D}_{\text{KL}}(\cdot \parallel \cdot)$ is the Kullback-Leibler divergence between two probability densities. One would like to minimize the function J over $\boldsymbol{\theta}$; if the family of maps $\mathbf{T}(\cdot, \boldsymbol{\theta})$ is rich enough, the KL divergence will approach zero and $\mathbf{T}_{\#} p_{\text{ref}} \approx p_{\text{target}}$.

In general, the family of maps $\mathbf{T}(\cdot, \boldsymbol{\theta})$ can contain any invertible function approximator that can be trained over $\boldsymbol{\theta}$ to push a treatable reference p_{ref} to the target p_{target} . Different choices for such a family have been proposed in the literature, e.g. polynomials regressors [20], Tensor-Train representations [9] and variational approximations [19, 4]. The accuracy of $\mathbf{T}_{\#} p_{\text{ref}}$ will depend on how well \mathbf{T} represents a map between the two densities. In this paper, we propose INNs as a suitable choice for \mathbf{T} that, at the same time, retains the universal approximation properties of deep neural networks and makes the minimization tractable because of the triangular architecture within the layers \mathbf{T}_ℓ . In fact, the main computational bottleneck in the minimization of the expression in (4) is that, as we will see, it involves the evaluation of $\log |\det \nabla \mathbf{T}|$ at every input of the training set and at every training step of the algorithm, which becomes quickly practically unfeasible. Lemma 1 showed how, for INNs, this expression can be calculated essentially at no extra cost during the forward pass.

Different algorithms can be constructed depending on the choices of p_{ref} and p_{target} . Although the ultimate goal is to sample from the posterior $p_{x|y}$, for some specific combination of densities p_{target}

¹For any invertible map \mathbf{T} and probability density p , the pushforward density of p is given by $\mathbf{T}_{\#} p(\mathbf{u}) = p(\mathbf{T}^{-1}(\mathbf{u})) |\det \nabla_{\mathbf{u}} \mathbf{T}^{-1}(\mathbf{u})|$.

and p_{ref} this can be done in two phases: first, train a transport map between the two densities; then, recover posterior samples via specific conditional procedures. We will study three cases, which are represented in Figure (2).

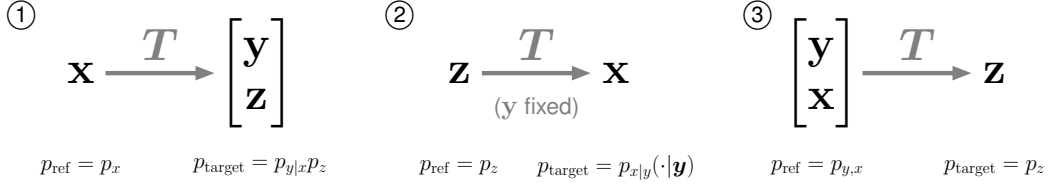


Figure 2: Transport schemes of the three considered cases

In both cases $\textcircled{1}$ and $\textcircled{3}$, the family of maps $\mathbf{T}(\cdot, \boldsymbol{\theta})$ is trained over $\boldsymbol{\theta}$ independently of the actual observation \mathbf{y} . After training is performed, samples from $p_{x|y}(\cdot|\mathbf{y})$ can be recovered for any contingent \mathbf{y} by a conditional procedure. When \mathbf{T} is taken to be an INN, case $\textcircled{1}$ corresponds to an extension of [1] to general likelihood functions $p_{y|x}$. Case $\textcircled{3}$ is related to [20], where families of polynomial maps \mathbf{T} are employed, and will be studied further in section 4. On the other hand, case $\textcircled{2}$ attempts to sample directly from the posterior $p_{y|x}(\cdot|\mathbf{y})$, therefore training requires the actual observation \mathbf{y} . For a different observation, training should be recomputed. Stein variational inference [19, 4] closely relates to this case. In the following theorem, for each case we derive an explicit loss upon which a family of maps $\mathbf{T}(\cdot, \boldsymbol{\theta})$ can be trained. Algorithms to sample from $p_{x|y}$ are given in appendix B.

Theorem 1. *Given a parametric family of invertible maps $\mathbf{T}(\cdot, \boldsymbol{\theta})$, minimizing the function $J(\boldsymbol{\theta})$ in (4) over $\boldsymbol{\theta}$ is equivalent to minimize the following losses $L(\boldsymbol{\theta})$:*

$\textcircled{1}$ *Let $\mathcal{X} \equiv \mathbb{R}^d$, $z \in \mathbb{R}^{d-m}$ and assume $m < d$. Let $p_{\text{ref}} = p_x$ and $p_{\text{target}} = p_{y|x}p_z$. Then*

$$L(\boldsymbol{\theta}) := \mathbb{E}_{\mathbf{x} \sim p_x} \left[\frac{1}{2\sigma_y^2} \|\mathbf{T}^y(\mathbf{x}) - \mathbf{F}(\mathbf{x})\|_2^2 + \frac{1}{2} \|\mathbf{T}(\mathbf{x})\|_2^2 - \log |\det \nabla \mathbf{T}(\mathbf{x})| \right], \quad (5)$$

where $\mathbf{T}(\mathbf{x}) = [\mathbf{T}^y(\mathbf{x}), \mathbf{T}^z(\mathbf{x})]$, with $\mathbf{T}^y(\mathbf{x}) \in \mathbb{R}^m$ and $\mathbf{T}^z(\mathbf{x}) \in \mathbb{R}^{d-m}$.

$\textcircled{2}$ *Let $\mathcal{X} \equiv \mathbb{R}^d$, $z \in \mathbb{R}^d$ and an observed \mathbf{y} . Let $p_{\text{ref}} = p_z$ and $p_{\text{target}} = p_{x|y}(\cdot|\mathbf{y})$. Then*

$$L(\boldsymbol{\theta}) := \mathbb{E}_{\mathbf{z} \sim p_z} \left[\frac{1}{2\sigma_y^2} \|\mathbf{y} - \mathbf{F}(\mathbf{T}(\mathbf{z}))\|_2^2 - \log p_x(\mathbf{T}(\mathbf{z})) - \log |\det \nabla \mathbf{T}(\mathbf{z})| \right]. \quad (6)$$

$\textcircled{3}$ *Let $\mathcal{X} \equiv \mathbb{R}^{m+d}$, $z \in \mathbb{R}^{m+d}$, $p_{\text{ref}} = p_{y,x}$ and $p_{\text{target}} = p_z$. Then*

$$L(\boldsymbol{\theta}) := \mathbb{E}_{\mathbf{w} \sim p_{y,x}} \left[\frac{1}{2} \|\mathbf{T}(\mathbf{w})\|_2^2 - \log |\det \nabla \mathbf{T}(\mathbf{w})| \right]. \quad (7)$$

A proof of Theorem 1 is given in appendix A. Here, we comment on the different losses. A summarized qualitative comparison can be found in Table 1 of appendix B.

Loss comparison. In practice, expectations within the losses of Theorem 1 should be approximated. A sensible choice is to exploit Monte Carlo samples, which can be directly obtained in each of the three cases and will play the role of training set for the family of maps $\mathbf{T}(\cdot, \boldsymbol{\theta})$. For both cases $\textcircled{1}$ and $\textcircled{3}$, these samples, together with potentially expensive evaluations of the model \mathbf{F} , can be performed *a priori* of the training phase. In addition, no gradient of \mathbf{F} is required during training, which allows \mathbf{F} to be completely treated as a black box. Vice versa, the loss in case $\textcircled{2}$ involve the term $\mathbf{F}(\mathbf{T}^y(\mathbf{z}))$, which does not allow offline evaluations of \mathbf{F} and requires its gradient during training.

The minimization of the first term in the loss of case $\textcircled{1}$ can be challenging. First, \mathbf{T}^y has to be trained to be a surrogate of \mathbf{F} , which can be difficult if \mathbf{F} is particularly complicated or exhibits an unstable (e.g. chaotic) behaviour. In addition, either if σ_y^2 is very small or m is very large, the loss can become very steep and difficult to optimize. Similar issues are present in case $\textcircled{2}$. In contrast, the loss in case $\textcircled{3}$ strikes for its simplicity. The first term in the loss pushes all samples towards the mode of the standard Gaussian density p_z , whereas the second term is a repulsion force that maintains the apart.

The information about the model and the probabilistic relation between hidden space and observation space is completely contained within the training set sampled from $p_{y,x}$.

Furthermore, we observe that, unlike in case ②, cases ① and ③ never require evaluations from the prior p_x but only samples from it. This makes them very suitable for sequential Bayesian inference, as we will study further in section 5.

In defence of case ②, if we want to sample from a specific posterior $p_{x|y}(\cdot|\mathbf{y})$ and if none of the issues raised above constitute a major difficulty, for particular applications this case may result faster than the other two, because the family of maps $\mathbf{T}(\cdot, \boldsymbol{\theta})$ is trained to map samples directly to the posterior. In addition, unlike ① and ③, case ② does not require an explicit expression for \mathbf{T}^{-1} .

4 HINT: Hierarchical Invertible Neural Transport

In this section, we propose an algorithm to sample from a posterior density $p_{x|y}$ via case ③, which we discussed to be appealing for several reasons.

4.1 From joint to posterior via Knothe-Rosenblatt transport maps

Consider an invertible transport map $\mathbf{T} : \mathbb{R}^{m+d} \rightarrow \mathbb{R}^{m+d}$ and suppose that it can be rewritten as a Knothe-Rosenblatt rearrangement, so that $\mathbf{T}(\mathbf{w}) := [\mathbf{T}^y(\mathbf{y}), \mathbf{T}^x(\mathbf{y}, \mathbf{x})]$ for $\mathbf{w} := [\mathbf{y}, \mathbf{x}] \in \mathbb{R}^{m+d}$, $\mathbf{T}^y(\mathbf{y}) \in \mathbb{R}^m$ and $\mathbf{T}^x(\mathbf{y}, \mathbf{x}) \in \mathbb{R}^d$. Let us denote by $\mathbf{S}(\mathbf{z}) := [\mathbf{S}^y(\mathbf{z}_y), \mathbf{S}^x(\mathbf{z}_y, \mathbf{z}_x)]$ its inverse, i.e. $\mathbf{S} = \mathbf{T}^{-1}$ and $\mathbf{S}^y = (\mathbf{T}^y)^{-1}$, for $\mathbf{z} := [\mathbf{z}_y, \mathbf{z}_x] \in \mathbb{R}^{m+d}$.

Observe that we can split the latent density as $p_z = p_{z_y} p_{z_x|z_y}$, where p_{z_y} and $p_{z_x|z_y}$ respectively correspond to the marginal density of \mathbf{z}_y and the conditional density of \mathbf{z}_x given \mathbf{z}_y . Because we chose p_z to be a standard Gaussian, we further have $p_{z_x} = p_{z_x|z_y}$. Finally, assume that $\mathbf{S}_{\#} p_z = p_{y,x}$ exactly, or equivalently $\mathbf{T}_{\#} p_{y,x} = p_z$. Then, it was shown in [20] that $\mathbf{S}_{\#}^y p_{z_y} = p_y$ and $\mathbf{S}_{\#}^x p_{z_x} = p_{x|y}$.

The result above suggests that, given a map \mathbf{T} satisfying the conditions above, a posterior sample $\mathbf{x} \sim p_{x|y}(\cdot|\mathbf{y})$ can be simply achieved by calculating $\mathbf{x} = \mathbf{S}^x([\mathbf{T}^y(\mathbf{y}), \mathbf{z}_x])$, for $\mathbf{z}_x \sim \mathcal{N}(\mathbf{0}, I)$. Intuitively, whereas the simple application of the map \mathbf{S}^x to a sample $\mathbf{z} = [\mathbf{z}_y, \mathbf{z}_x] \sim \mathcal{N}(\mathbf{0}, I)$ would provide a sample from the joint $p_{y,x}$, the act of fixing \mathbf{z}_y to be the anti-image of \mathbf{y} through \mathbf{T}^y makes sure that the resulting sample \mathbf{x} comes from the posterior $p_{x|y}$. A simplified visualization of this procedure is displayed in Figure 3.

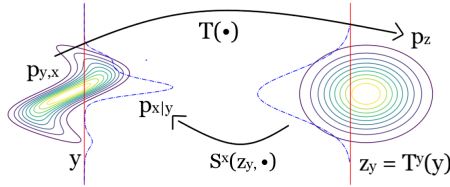


Figure 3: Contours of joint and reference densities. Given data \mathbf{y} (left red line) and its anti-image $\mathbf{z}_y = \mathbf{T}^y(\mathbf{y})$ (right red line), $\mathbf{S}^x(\mathbf{z}_y, \cdot)$ maps a marginal Gaussian sample to the posterior (dashed).

4.2 Hierarchical architecture

The goal is to introduce an architecture which endows \mathbf{T} with a Knothe-Rosenblatt structure in order to apply the sampling procedure described in section 4.1. In fact, such a structure is not satisfied by a general INN architecture in (1) because of the orthogonal transformations Q_ℓ , which are essential to have a large representation power of the network. In order to overcome this issue, we proceed as follows: first, we develop a hierarchical generalization of the architecture in (1) to embed a rich input-to-output dependence within each layer \mathbf{T}_ℓ ; then, we enforce the last level of each hierarchy to be triangular, so that the overall map \mathbf{T} satisfies the desired structure.

Intuitively, we want to recursively nest INNs within each other in order to perform multiple coordinate splittings and therefore densify the architecture structure. In order to characterize this nesting procedure, for each layer ℓ we define a binary tree \mathcal{H}_ℓ of splittings. Each entry $h \in \mathcal{H}_\ell$ refers to a splitting coordinate and to the sub-tree of its children. We denote the tree root by $\tilde{h} \in \mathcal{H}_\ell$. Given h , let us denote by h^- and h^+ its direct children. Also, we denote by $H := |\mathcal{H}_\ell|$ the cardinality of the

tree, i.e. the number of splittings. Let us define the following *hierarchical architecture*:

$$\mathbf{T}_{\ell,h}(\mathbf{u}) := \left[\mathbf{T}_{\ell,h^+}^2(\tilde{\mathbf{u}}_2) \odot \exp(\mathbf{s}_{\ell,h}(\tilde{\mathbf{u}}_1)) + \mathbf{t}_{\ell,h}(\tilde{\mathbf{u}}_1) \right], \quad \text{with } \tilde{\mathbf{u}} := \begin{bmatrix} \tilde{\mathbf{u}}_1 \\ \tilde{\mathbf{u}}_2 \end{bmatrix} := Q_{\ell,h} \mathbf{u}, \quad (8)$$

with the initial condition $\mathbf{T}_{\ell,h}(\mathbf{u}) := \mathbf{u}$ for $h = \emptyset$. $Q_{\ell,h}$ is an arbitrary orthogonal matrix, whereas $\mathbf{s}_{\ell,h}$ and $\mathbf{t}_{\ell,h}$ are arbitrarily complex neural networks. Note that, for $H = 1$, (8) corresponds to (1). Figure 4a displays the architecture of a hierarchical layer $\mathbf{T}_{\ell,h}$, whereas Figure 4b shows the layout of the Jacobian $\nabla \mathbf{T}_{\ell,\tilde{h}}(\mathbf{u})$ for a tree \mathcal{H}_ℓ with $H = 3$, with respect to the transformed inputs $Q_{\ell,\tilde{h}^-} \tilde{\mathbf{u}}_1$ and $Q_{\ell,\tilde{h}^+} \tilde{\mathbf{u}}_2$. Analogously to hierarchical matrices, the architecture in (8) densifies the dependence between input and output of $\mathbf{T}_{\ell,\tilde{h}}$ by recursively nesting INNs layers within themselves.

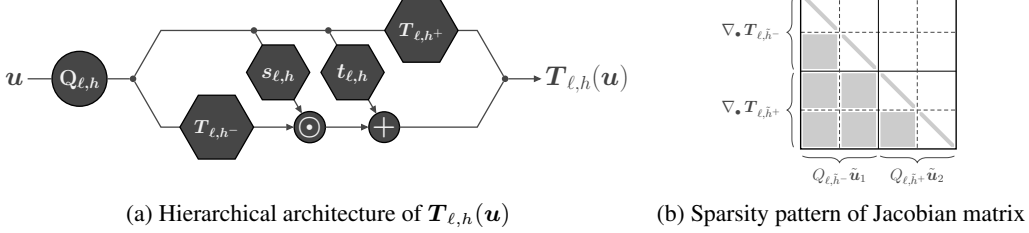


Figure 4

Let us define $\mathbf{T}_\ell := \mathbf{T}_{\ell,\tilde{h}}$ and the overall map $\mathbf{T} := \mathbf{T}_L \circ \dots \circ \mathbf{T}_1$. It is easy to check that $\log |\det \nabla \mathbf{T}|$ can be recursively decomposed to assume a similar structure as in Lemma 1 and calculated essentially for free during the forward pass.

Given the hierarchical construction of \mathbf{T}_ℓ defined above, we can enforce the overall map \mathbf{T} to retain the desired Knothe-Rosenblatt structure by, for each $\ell = 1, \dots, L$: (a) defining \tilde{h} to split between the variables \mathbf{y} and \mathbf{x} ; (b) taking $Q_{\ell,\tilde{h}} = I$. It immediately follows that, for any input $\mathbf{w} = [\mathbf{y}, \mathbf{x}]$, we can split $\mathbf{T}(\mathbf{w}) := [\mathbf{T}^y(\mathbf{y}), \mathbf{T}^x(\mathbf{y}, \mathbf{x})]$, with $\mathbf{T}^y(\mathbf{y}) \in \mathbb{R}^m$ and $\mathbf{T}^x(\mathbf{y}, \mathbf{x}) \in \mathbb{R}^d$. Hence, after training is performed upon the loss in (7), we can apply the procedure described in section 4.1 to sample from a posterior density $p_{\mathbf{x}|\mathbf{y}}$. We address the overall algorithm as *Hierarchical Invertible Neural Transport* (HINT). An implementation is given in appendix B.

5 HINT for sequential Bayesian inference

Sequential Bayesian inference typically describes a dynamical framework where data arrives in a streaming form. We denote by $\mathbf{y}_{1:t}$ a sequence of data points $\mathbf{y}_1, \dots, \mathbf{y}_t$ at times $1, \dots, t$. Analogously, we assume that there is an underlying sequence of correspondent hidden states $\mathbf{x}_{1:t}$. Model dependencies are defined through the graphical model in Figure 8.

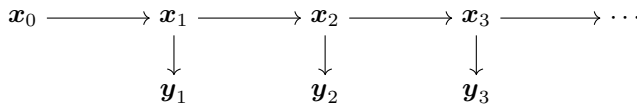


Figure 6: Dependence structure in sequential Bayesian framework

By Bayes' theorem and the assumed dependence structure, we have

$$p_{x_t|y_{1:t}}(\mathbf{x}_t|\mathbf{y}_{1:t}) \propto p_{y_t|x_t}(\mathbf{y}_t|\mathbf{x}_t)p_{x_t|y_{1:t-1}}(\mathbf{x}_t|\mathbf{y}_{1:t-1}), \quad (9)$$

$$p_{x_t|y_{1:t-1}}(\mathbf{x}_t|\mathbf{y}_{1:t-1}) = \mathbb{E}_{\mathbf{x}_{t-1} \sim p_{x_{t-1}|y_{1:t-1}}} [p_{x_t|x_{t-1}}(\mathbf{x}_t|\mathbf{x}_{t-1})]. \quad (10)$$

Equation (10) is usually known as the prediction step, while equation (9) is called assimilation (or updating) step. Here, $p_{x_t|y_t}$ is the desired posterior density, $p_{y_t|x_t}$ is the likelihood function, whereas $p_{x_t|y_{1:t-1}}$ plays the role of prior density given the previous observations $\mathbf{y}_{1:t-1}$. The analytic expression of the prior is not given explicitly, but rather through an expectation over the previous posterior $p_{x_{t-1}|y_{1:t-1}}$. If we have samples from the previous posterior, we can estimate the expectation via Monte Carlo, however this can easily be very inaccurate if the transition density

$p_{x_t|x_{t-1}}$ is complicated or very concentrated. In the limit case where the relation between x_{t-1} and x_t is deterministic, i.e. $p_{x_t|x_{t-1}}$ is a Dirac delta function, a Monte Carlo estimate is not even possible. In addition to this problematic, in many applications of interest, every evaluation of the transition density requires the solution of a very expensive model, and the evaluation of the prior density through a Monte Carlo approximation would become too expensive for online prediction.

For those reasons, we would like to have an algorithm that is able to sequentially generate samples from the posterior $p_{x_t|y_{1:t}}$ but does not need to evaluate the prior density $p_{x_t|y_{1:t-1}}$. Theorem 2 shows how to generalize the results for HINT (case ③) in Theorem 1 to sequential Bayesian inference and how only samples from $p_{x_t|y_{1:t-1}}$ are required, but never an analytical evaluation of it. An analogous result can be derived for case ①. As before, although the results can be achieved for general probability densities, we focus on additive Gaussian noise relations $x_t := M(x_{t-1}) + \sigma_x \eta$ and $y := F(x_t) + \sigma_y \xi$, for some non-linear operators $M : \mathbb{R}^d \rightarrow \mathbb{R}^d$, $F : \mathbb{R}^d \rightarrow \mathbb{R}^m$, some standard Gaussian noises η, ξ and standard deviations σ_x and σ_y . This immediately implies $p_{x_t|x_{t-1}}(\cdot|x_{t-1}) = \mathcal{N}(M(x_{t-1}), \sigma_x^2 I)$ and $p_{y_t|x_t}(\cdot|x_t) = \mathcal{N}(F(x_t), \sigma_y^2 I)$.

Theorem 2. *Let $T(\cdot; \theta)$ be a parametric family of invertible transport map from \mathbb{R}^{m+d} to \mathbb{R}^{m+d} . Suppose we observed $\mathbf{y}_{1:t-1}$ and denote $p_{y_t, x_t|y_{1:t-1}} = p_{y_t, x_t|y_{1:t-1}}(\cdot|\mathbf{y}_{1:t-1})$. Let us define*

$$J_t : \mathbb{R}^n \rightarrow [0, \infty) : \theta \mapsto \mathcal{D}_{\text{KL}}(\mathbf{T}_{\#} p_{y_t, x_t|y_{1:t-1}} \| p_z). \quad (11)$$

Then, minimizing $J_t(\theta)$ in (11) over θ is equivalent to minimize the following loss:

$$L_t(\theta) := \mathbb{E}_{\mathbf{w}_t \sim p_{y_t, x_t|y_{1:t-1}}} \left[\frac{1}{2} \|\mathbf{T}(\mathbf{w}_t)\|_2^2 - \log |\det \nabla \mathbf{T}(\mathbf{w}_t)| \right]. \quad (12)$$

A proof follows directly from the proof of Theorem 1 in appendix A. Importantly, the minimization of the loss in (12) at time t should be initialized at the optimal value of θ at time $t-1$. In fact, if the geometry of the posterior does not change much, the new optimal value is going to be close to the previous one, and the training very short.

6 Numerical experiments

In this section, we compare the performance of standard INN (case ①) and HINT (case ③) on two challenging numerical experiments in a Bayesian inference framework. In both cases, we use approximately $n = 10^6$ parameters. We use HINT with a coarse hierarchical depth $H = 3$ and show that this suffices to compare favorably to INN.

6.1 Competitive Lotka-Volterra and unobserved species prediction over time

Competitive Lotka-Volterra is a generalization of the classic Lotka-Volterra which describes the demographical interaction of d species competing on common resources. It is given by

$$\frac{du_i}{dt} = r_i u_i \left(1 - \sum_{j=1}^d \alpha_{ij} u_j \right) \quad (13)$$

for $i = 1, \dots, d$, where u_i is the size of the i -th species at a given time, r_i is its growth rate and α_{ij} describes the interaction with the other species. We take $d = 4$ and set parameters $r_i, \alpha_{ij} \sim \mathcal{N}(1, 0.3^2)$. Observations are taken at times $t_j = j$, for $j = 1, \dots, 10$, and we set $t_0 = 0$. The solution of (13) between $[t_{j-1}, t_j]$ characterizes the transition model M , and $\mathbf{x}(t_j) = M(\mathbf{x}(t_{j-1})) + \sigma_x \eta$, where $\sigma_x = 10^{-2}$ and $\eta \sim \mathcal{N}(\mathbf{0}, I)$. We observe a perturbed number of the first three species $\mathbf{y}_{t_j} = F(\mathbf{x}^{\text{true}}(t_j)) + \sigma_y \xi_{t_j}$ with $F(\mathbf{x}(t)) := \mathbf{x}_{1:3}(t)$ and $\sigma_y = 10^{-1}$, where $\mathbf{x}^{\text{true}}(t)$ is a realization of the process $\mathbf{x}(t)$ with $\mathbf{x}^{\text{true}}(0) \sim \mathcal{N}(\mathbf{1}, 10^{-4}I)$. We set an initial prior $\mathbf{x}(0) \sim \mathcal{N}(\mathbf{1}, 10^{-2}I)$. The goal is to sequentially recover the posterior densities and to predict the unobserved component x_4 .

At $t_1 = 1$, we estimate the mean-squared-error (MSE) of the trace of the posterior covariance matrix both varying the number of training samples and training steps. Figure 7 (top row) shows that both standard INN and HINT converge to very small values of the MSE. INN appears to largely struggle for small training sizes, but seems to perform slightly better for many training epochs.

Figure 7 (bottom row) describes the sequential prediction of x_4 , which shows a largely better performance of HINT over INN. Methods were trained with 64000 samples for 50 epochs.

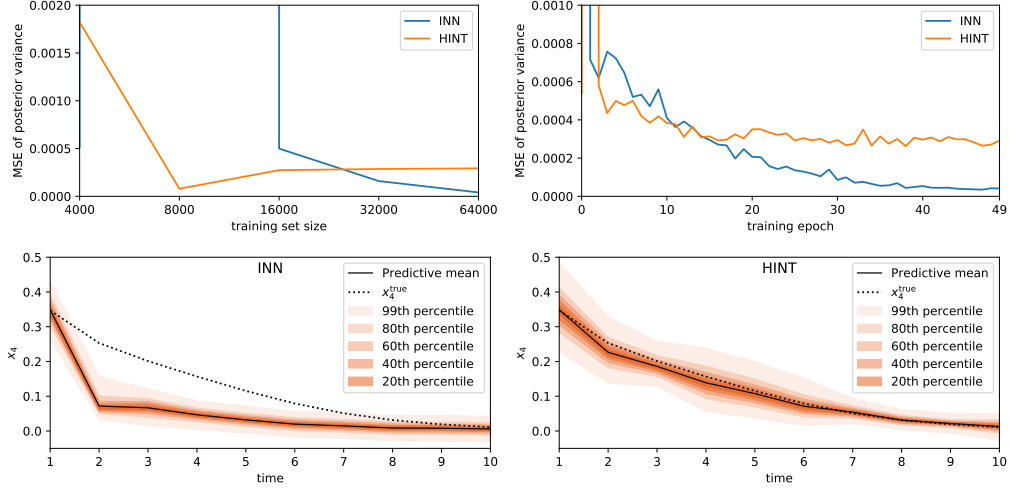


Figure 7: MSE comparisons and prediction of x_4 for INN and HINT

6.2 Lorenz96 transition and log-Rosenbrock observation models

Lorenz96 is a chaotic dynamical system characterized by

$$\frac{du_i}{dt} = (u_{i+1} - u_{i-2})u_{i-1} - u_i + \alpha, \quad (14)$$

for $i = 1, \dots, d$, where it is assumed that $u_{-1} = u_{d-1}$, $u_0 = u_d$ and $u_{d+1} = u_1$. We take $d = 40$ and set $\alpha = 8$ (chaotic regime). We start at $t_0 = 0$ and take an observation at time $t_1 = \frac{1}{10}$. The solution of (14) between $[0, t_1]$ characterizes the transition model \mathcal{M} , and $\mathbf{x}(t_1) = \mathcal{M}(\mathbf{x}(0)) + \sigma_x \boldsymbol{\eta}$, where $\sigma_x = 10^{-1}$ and $\boldsymbol{\eta} \sim \mathcal{N}(\mathbf{0}, I)$. To make the problem very complicated, we take $\mathbf{F} \in \mathbb{R}^{39}$ to be a log-Rosenbrock function in each component, i.e. $F_i(\mathbf{x}) = \log(100(x_{i+1} - x_i^2)^2 + (1 - x_i)^2)$ for $i = 1, \dots, 39$, and observe $\mathbf{y}_{t_1} = \mathbf{F}(\mathbf{x}^{\text{true}}(t_1)) + \sigma_y \boldsymbol{\xi}_{t_1}$ with $\sigma_y = 10^{-1}$, where $\mathbf{x}^{\text{true}}(t)$ is a realization of the process $\mathbf{x}(t)$ with $\mathbf{x}^{\text{true}}(0) \sim \mathcal{N}(\mathbf{1}, 10^{-4}I)$. We set an initial prior $\mathbf{x}(0) \sim \mathcal{N}(\mathbf{1}, I)$. The goal is to sample from the posterior at time t_1 .

For this hard experiment, INN failed to produce meaningful results. We remark that with better annealing rate of σ_y and network configurations, INN may still be able to converge, but this can be tedious and difficult. In contrast, HINT does not have to worry about concentration issues, as highlighted in section 3. Hence, it is much more robust and, importantly, requires much less parameters tweaking. Figure 9 shows its convergence at time t_1 .

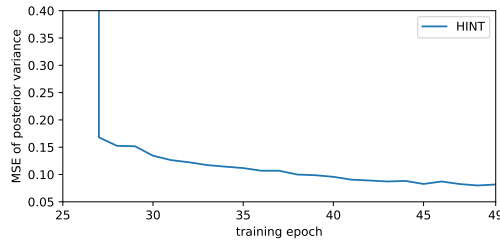


Figure 9: MSE of the trace of the poster covariance over training epochs

7 Conclusion

In this work, we introduced HINT as an algorithm that combines INNs and optimal transport to sample from a posterior distribution in a general and a sequential Bayesian framework. We discussed how the use of HINT over INN can be advantageous for several reasons, and we performed numerical comparisons in two challenging test cases. Further research directions may include the use of Quasi-Monte Carlo training samples for better space-filling and generalization properties [6], and multilevel techniques to beat down the computation cost of generating the training set [18].

A Appendix: Proofs

Proof of Lemma 1. With the notation above, we have $\tilde{\mathbf{u}}^{\ell-1} = Q_\ell^\top \mathbf{u}^{\ell-1}$. Then, by chain rule we have

$$\begin{aligned}
\log |\det \nabla_{\mathbf{u}} \mathbf{T}(\mathbf{u})| &= \log \left| \det \left(\prod_{\ell=1}^L \nabla_{\mathbf{u}^{\ell-1}} \mathbf{T}_\ell(\mathbf{u}^{\ell-1}) \right) \right| \\
&= \log \left| \det \left(\prod_{\ell=1}^L \nabla_{\tilde{\mathbf{u}}^{\ell-1}} \mathbf{T}_\ell(\mathbf{u}^{\ell-1}) Q_\ell \right) \right| \\
&= \log \left| \prod_{\ell=1}^L (\det \nabla_{\tilde{\mathbf{u}}^{\ell-1}} \mathbf{T}_\ell(\mathbf{u}^{\ell-1}) \det Q_\ell) \right| \\
&= \log \left(\prod_{\ell=1}^L \text{prod} \left(\exp(\mathbf{s}(\tilde{\mathbf{u}}_1^{\ell-1})) \right) \right) \\
&= \sum_{\ell=1}^L \text{sum}(\mathbf{s}(\tilde{\mathbf{u}}_1^{\ell-1})),
\end{aligned}$$

where we denote by $\text{prod}(\cdot)$ the element-wise product and we used that $\det Q_\ell = 1$ because Q_ℓ are orthogonal matrices. \square

Proof of Theorem 1. Let us take a family of invertible maps $\mathbf{T}(\cdot) := \mathbf{T}(\cdot; \boldsymbol{\theta})$. It is easy to check that

$$\mathcal{D}_{\text{KL}}(\mathbf{T} \# p_{\text{ref}} \parallel p_{\text{target}}) = \mathcal{D}_{\text{KL}}(p_{\text{ref}} \parallel (\mathbf{T}^{-1}) \# p_{\text{target}}) = -\mathbb{E}_{p_{\text{ref}}} \left[\log(p_{\text{target}} \circ \mathbf{T}) + \log |\det \nabla \mathbf{T}| \right] + \text{const},$$

for any densities p_{ref} and p_{target} , with $\text{const} = \mathbb{E}_{p_{\text{ref}}}[\log p_{\text{ref}}]$. We study the following three cases separately.

- ① Let $\mathcal{X} \equiv \mathbb{R}^d$, assume $m < d$ and take $\mathbf{z} \in \mathbb{R}^{d-m}$. Let $p_{\text{ref}} = p_x$ and $p_{\text{target}} = p_{y|x} p_z$. We observe that the decomposition of the target density as $p_{y|x} p_z$ is enforcing independence of \mathbf{z} from \mathbf{y} and \mathbf{x} , in fact $p_{\text{target}} = p_{y,z|x} = p_{y|x} p_{z|y,x} = p_{y|x} p_z$. Then

$$p_{\text{target}}(\mathbf{T}(\mathbf{x})) = p_{y|x}(\mathbf{T}^y(\mathbf{x})) p_z(\mathbf{T}^z(\mathbf{x})),$$

where $\mathbf{T}(\mathbf{x}) = [\mathbf{T}^y(\mathbf{x}), \mathbf{T}^z(\mathbf{x})]$, with $\mathbf{T}^y(\mathbf{x}) \in \mathbb{R}^m$ and $\mathbf{T}^z(\mathbf{x}) \in \mathbb{R}^{d-m}$. By definitions of p_{ref} , p_{target} , $p_{y|x}$ and p_z , we have

$$\begin{aligned}
-\mathbb{E}_{p_{\text{ref}}}[\log p_{\text{target}} \circ \mathbf{T}] &= -\mathbb{E}_{\mathbf{x} \sim p_x} [\log p_{y|x}(\mathbf{T}^y(\mathbf{x})|\mathbf{x}) + \log p_z(\mathbf{T}^z(\mathbf{x}))] \\
&= \mathbb{E}_{\mathbf{x} \sim p_x} \left[\frac{1}{2\sigma_y^2} \|\mathbf{T}^y(\mathbf{x}) - \mathbf{F}(\mathbf{x})\|_2^2 + \frac{1}{2} \|\mathbf{T}(\mathbf{x})\|_2^2 \right] + \text{const}.
\end{aligned}$$

Hence, minimizing $\mathcal{D}_{\text{KL}}(\mathbf{T} \# p_x \parallel p_{y|x} p_z)$ with respect to $\boldsymbol{\theta}$ is equivalent to minimize the following loss function:

$$L(\boldsymbol{\theta}) = \mathbb{E}_{\mathbf{x} \sim p_x} \left[\frac{1}{2\sigma_y^2} \|\mathbf{T}^y(\mathbf{x}) - \mathbf{F}(\mathbf{x})\|_2^2 + \frac{1}{2} \|\mathbf{T}(\mathbf{x})\|_2^2 - \log |\det \nabla \mathbf{T}(\mathbf{x})| \right].$$

- ② Let $\mathcal{X} \equiv \mathbb{R}^d$, $\mathbf{z} \in \mathbb{R}^d$ and suppose we observed \mathbf{y} . Let $p_{\text{ref}} = p_z$ and $p_{\text{target}} = p_{x|y}(\cdot|\mathbf{y})$. By Bayes' theorem and our likelihood definition, we can rewrite

$$-\log p_{x|y}(\mathbf{T}(\mathbf{z})|\mathbf{y}) = \frac{1}{2\sigma_y^2} \|\mathbf{y} - \mathbf{F}(\mathbf{T}(\mathbf{z}))\|_2^2 - \log p_x(\mathbf{T}(\mathbf{z})) + \text{const}.$$

Hence, minimizing $\mathcal{D}_{\text{KL}}(\mathbf{T} \# p_z \parallel p_{x|y})$ with respect to $\boldsymbol{\theta}$ is equivalent to minimize the following loss function:

$$L(\boldsymbol{\theta}) = \mathbb{E}_{\mathbf{z} \sim p_z} \left[\frac{1}{2\sigma_y^2} \|\mathbf{y} - \mathbf{F}(\mathbf{T}(\mathbf{z}))\|_2^2 - \log p_x(\mathbf{T}(\mathbf{z})) - \log |\det \nabla \mathbf{T}(\mathbf{z})| \right].$$

- ③ Let $\mathcal{X} \equiv \mathbb{R}^{m+d}$, $\mathbf{z} \in \mathbb{R}^{m+d}$, $p_{\text{ref}} = p_{y,x}$ and $p_{\text{target}} = p_z$. Because we assumed p_z to be a standard Gaussian density, we have

$$-\log p_z(\mathbf{T}(\mathbf{x})) = \frac{1}{2} \|\mathbf{T}(\mathbf{x})\|_2^2 + \text{const}.$$

Hence, minimizing $\mathcal{D}_{\text{KL}}(\mathbf{T}_{\#} p_{y|x} \| p_z)$ with respect to $\boldsymbol{\theta}$ is equivalent to minimize the following loss function:

$$L(\boldsymbol{\theta}) = \mathbb{E}_{\mathbf{w} \sim p_{y,x}} \left[\frac{1}{2} \|\mathbf{T}(\mathbf{w})\|_2^2 - \log |\det \nabla \mathbf{T}(\mathbf{w})| \right].$$

□

B Appendix: Algorithms

	Case ①	Case ②	Case ③
Sensitivity to $\sigma_y \ll 1$	Sensitive	Sensitive	Not sensitive
Sensitivity to $m \gg 1$	Sensitive	Sensitive	Not sensitive
Observed data during training	Not required	Required	Not required
Model evaluations	Offline	Online	Offline
Gradient of the model	Not required	Required	Not required
Prior evaluations	Not required	Required	Not required
Explicit inverse map	Required	Not required	Required

Table 1: Qualitative summary of comparison between cases ①, ② and ③

Algorithm 1: Sampling from $p_{x|y}$ via ①

Input : \mathbf{y} , N_{train} , N_{out}

Output : $(\mathbf{x}^{(k)})_{k=1}^{N_{\text{out}}} \sim p_{x|y}$

- 1: Sample inputs $(\mathbf{x}^{(k)})_{k=1}^{N_{\text{train}}} \sim p_x$ and estimate the loss in (5)
 - 2: Train an INN $\mathbf{T}(\cdot; \boldsymbol{\theta})$ with the estimated loss and denote the minimizer by $\boldsymbol{\theta}^*$
 - 3: Sample $(\mathbf{z}^{(k)})_{k=1}^{N_{\text{out}}} \sim \mathcal{N}(\mathbf{0}, I)$
 - 4: Get $\mathbf{x}^{(k)} = \mathbf{S}([\mathbf{y}, \mathbf{z}^{(k)}]; \boldsymbol{\theta}^*) \sim p_{x|y}$, for $k = 1, \dots, N_{\text{out}}$, where $\mathbf{S} = \mathbf{T}^{-1}$
-

Algorithm 2: Sampling from $p_{x|y}$ via ②

Input : \mathbf{y} , N

Output : $(\mathbf{x}^{(k)})_{k=1}^N \sim p_{x|y}$

- 1: Sample inputs $(\mathbf{z}^{(k)})_{k=1}^N \sim \mathcal{N}(\mathbf{0}, I)$ and estimate the loss in (6)
 - 2: Train an INN $\mathbf{T}(\cdot; \boldsymbol{\theta})$ with the estimated loss and denote the minimizer by $\boldsymbol{\theta}^*$
 - 3: Get $\mathbf{x}^{(k)} = \mathbf{T}(\mathbf{z}^{(k)}; \boldsymbol{\theta}^*) \sim p_{x|y}$, for $k = 1, \dots, N$
-

Algorithm 3: Sampling from $p_{x|y}$ via ③ (HINT)

Input : $\mathbf{y}, N_{\text{train}}, N_{\text{out}}$ **Output :** $(\mathbf{x}^{(k)})_{k=1}^{N_{\text{out}}} \sim p_{x|y}$

- 1: Sample inputs $(\mathbf{w}^{(k)})_{k=1}^{N_{\text{train}}} \sim p_{y,x}$ via Algorithm 4 and estimate the loss in (7)
 - 2: Train an INN $\mathbf{T}(\cdot; \boldsymbol{\theta})$ with the estimated loss and denote the minimizer by $\boldsymbol{\theta}^*$
 - 3: Get $\mathbf{z}_y = \mathbf{T}^y(\mathbf{y})$
 - 4: Sample $(\mathbf{z}_x^{(k)})_{k=1}^{N_{\text{out}}} \sim \mathcal{N}(\mathbf{0}, \mathbf{I})$
 - 5: Get $\mathbf{x}^{(k)} = \mathbf{S}([\mathbf{z}_y, \mathbf{z}_x^{(k)}]; \boldsymbol{\theta}^*) \sim p_{x|y}$, for $k = 1, \dots, N_{\text{out}}$, where $\mathbf{S} = \mathbf{T}^{-1}$
-

Algorithm 4: Sampling $\mathbf{w} \sim p_{y,x}$

- 1: Sample $\mathbf{x} \sim p_x$
 - 2: Sample $\boldsymbol{\xi} \sim \mathcal{N}(\mathbf{0}, \mathbf{I})$
 - 3: Set $\mathbf{y} = \mathbf{F}(\mathbf{x}) + \sigma_y \boldsymbol{\xi} \sim p_{y|x}$
 - 4: Set $\mathbf{w} = [\mathbf{y}, \mathbf{x}] \sim p_{y,x}$
-

References

- [1] Lynton Ardizzone et al. “Analyzing inverse problems with invertible neural networks”. In: *arXiv preprint arXiv:1808.04730* (2018).
- [2] David M Blei, Alp Kucukelbir, and Jon D McAuliffe. “Variational inference: A review for statisticians”. In: *Journal of the American Statistical Association* 112.518 (2017), pp. 859–877.
- [3] Peng Chen et al. “Projected Stein Variational Newton: A Fast and Scalable Bayesian Inference Method in High Dimensions”. In: *arXiv preprint arXiv:1901.08659* (2019).
- [4] Gianluca Detommaso et al. “A Stein variational Newton method”. In: *Advances in Neural Information Processing Systems*. 2018, pp. 9187–9197.
- [5] Gianluca Detommaso et al. “Stein Variational Online Changepoint Detection with Applications to Hawkes Processes and Neural Networks”. In: *arXiv preprint arXiv:1901.07987* (2019).
- [6] Josef Dick, Frances Y Kuo, and Ian H Sloan. “High-dimensional integration: the quasi-Monte Carlo way”. In: *Acta Numerica* 22 (2013), pp. 133–288.
- [7] Laurent Dinh, David Krueger, and Yoshua Bengio. “Nice: Non-linear independent components estimation”. In: *arXiv preprint arXiv:1410.8516* (2014).
- [8] Laurent Dinh, Jascha Sohl-Dickstein, and Samy Bengio. “Density estimation using real nvp”. In: *arXiv preprint arXiv:1605.08803* (2016).
- [9] Sergey Dolgov et al. “Approximation and sampling of multivariate probability distributions in the tensor train decomposition”. In: *arXiv preprint arXiv:1810.01212* (2018).
- [10] Arnaud Doucet and Adam M Johansen. “A tutorial on particle filtering and smoothing: Fifteen years later”. In: *Handbook of nonlinear filtering* 12.656-704 (2009), p. 3.
- [11] Tarek A El Moselhy and Youssef M Marzouk. “Bayesian inference with optimal maps”. In: *Journal of Computational Physics* 231.23 (2012), pp. 7815–7850.
- [12] Walter R Gilks, Sylvia Richardson, and David Spiegelhalter. *Markov chain Monte Carlo in practice*. Chapman and Hall/CRC, 1995.
- [13] Aidan N Gomez et al. “The reversible residual network: Backpropagation without storing activations”. In: *Advances in neural information processing systems*. 2017, pp. 2214–2224.
- [14] Chin-Wei Huang et al. “Neural autoregressive flows”. In: *arXiv preprint arXiv:1804.00779* (2018).
- [15] Jörn-Henrik Jacobsen, Arnold Smeulders, and Edouard Oyallon. “i-revnet: Deep invertible networks”. In: *arXiv preprint arXiv:1802.07088* (2018).
- [16] Durk P Kingma and Prafulla Dhariwal. “Glow: Generative flow with invertible 1x1 convolutions”. In: *Advances in Neural Information Processing Systems*. 2018, pp. 10236–10245.
- [17] Durk P Kingma et al. “Improved variational inference with inverse autoregressive flow”. In: *Advances in neural information processing systems*. 2016, pp. 4743–4751.

- [18] Frances Kuo et al. “Multilevel quasi-Monte Carlo methods for lognormal diffusion problems”. In: *Mathematics of Computation* 86.308 (2017), pp. 2827–2860.
- [19] Qiang Liu and Dilin Wang. “Stein variational gradient descent: A general purpose bayesian inference algorithm”. In: *Advances In Neural Information Processing Systems*. 2016, pp. 2378–2386.
- [20] Youssef Marzouk et al. “Sampling via measure transport: An introduction”. In: *Handbook of Uncertainty Quantification* (2016), pp. 1–41.
- [21] George Papamakarios, Theo Pavlakou, and Iain Murray. “Masked autoregressive flow for density estimation”. In: *Advances in Neural Information Processing Systems*. 2017, pp. 2338–2347.
- [22] Manuel Pulido and Peter Jan vanLeeuwen. “Kernel embedding of maps for sequential Bayesian inference: The variational mapping particle filter”. In: *arXiv preprint arXiv:1805.11380* (2018).
- [23] Christian Robert and George Casella. *Monte Carlo statistical methods*. Springer Science & Business Media, 2013.
- [24] Josef Stoer and Roland Bulirsch. *Introduction to numerical analysis*. Vol. 12. Springer Science & Business Media, 2013.
- [25] Cédric Villani. *Optimal transport: old and new*. Vol. 338. Springer Science & Business Media, 2008.